

## Photocatalytic Homogeneous and Heterogeneous Processes for Polluted Water from the Northern Oilfields in Iraq

Ruya Yilmaz Saber<sup>1\*</sup>, Mohammed Jaafar Alatabe<sup>1</sup>, Nagham Obaid Karim<sup>1</sup>

<sup>1</sup> Department of Environmental Engineering, College of Engineering, Mustansiriya University, P.O. Box 14150, Babal-Mu'adhem, Baghdad, Iraq

\* Corresponding author's e-mail: [ecma012@uomustansiriya.edu.iq](mailto:ecma012@uomustansiriya.edu.iq)

### ABSTRACT

Produced water is one of the most dangerous types of pollution for the environment, specifically the soil, since it is full of oil, suspended particulates, dissolved compounds, and various other pollutants. This research describes the advanced oxidation process (AOPs) that were studied to purge the generated water from the Al Khabaz oil-field located in (Northern Iraq – Kirkuk governorate) of any oil content using two photocatalytic homogeneous and heterogeneous processes in the batch system under optimal conditions: homogeneous processes, including Photo-Fenton (hydrogen peroxide, ferrous sulfates, and ultraviolet light), and Fenton process (hydrogen peroxide, and ferrous sulfates), and Direct-Photolysis (ultraviolet only) were used to study the effects of hydrogen peroxide ( $H_2O_2$ ) & ferrous sulfate ( $Fe^{+2}$ ), doses, irradiation time, pH Value, and intensity of UV to the oil removal efficiency. This work investigated the maximum efficiency in Photo Fenton = 85.68%, in Fenton = 75.01%, and in direct UV photolysis = 56.64%. The heterogeneous photocatalytic process ( $TiO_2/UV$ ) studied the effect of titanium dioxide ( $TiO_2$ ) nanoparticles doses and UV intensity. The results show that the optimal efficiency achieved was 60.95%. X-ray diffraction (XRD), scanning electron microscopy (SEM), and Fourier Transforms Infrared Spectroscopy (FT-IR) were used to look into the characteristics of the catalyst titanium dioxide nanoparticles.  $TiO_2$  NPs seemed to be spherical in the SEM test, and their FT-IR analysis absorption values ranged from 424.77 to 3403.71  $cm^{-1}$ . Their sizes varied between 31.57 and 38.40 nm, and XRD revealed details regarding their chemical composition.

**Keywords:** advanced oxidation processes (AOPs), produced water, oil content, photocatalytic, homogeneous and heterogeneous.

### INTRODUCTION

The wastewater produced during crude oil extraction processes is known as produced water (PW). When this water is brought to the surface, it contains complex pollutants such as scattered and dissolved organic and inorganic compounds (Mohanakrishna et al., 2021). Toxic and dangerous pollutants, such as organic matter, dissolved salts, and natural minerals, exist in the produced water, causing risks to public health and the environment (Rana et al., 2021). The pollutants of produced water consist of many toxic materials, inorganic, and organic components such as (oils, grease, phenols, Sulfate, phosphate, salts, minerals, and heavy materials); due to its dangerous nature, wastewater polluted with oil can cause significant

environmental issues (Villegas et al., 2016)(Mustafa et al., 2013). Oily-produced water contains aliphatic, aromatic, and phenols, so the removal processes from wastewater is a global concern since they are deemed carcinogenic and hazardous to the ecosystem and public health (Villegas et al., 2016; Tetteh et al., 2020). For recycling and reuse, this sort of wastewater management requires affordable and environmentally beneficial ways of treatment. A strategy that can be used is a three-tiered water hierarchy: reduction, disposal, as well as preparation for reuse and recycling.

There are many ways to treat this type of water; for the separation of organic content from generated water, a variety of approaches are available, including coagulation (Jabbar and Alatabe, 2021; Hadi et al., 2020), adsorption (Alatabe et

al., 2021), biological separation (Lekomtsev et al., 2021), and membrane separation (Shawkat et al., 2016). None of these treatment methods, however, adequately treats the produced water. Advanced oxidation processes are a different stage of treatment that is optional (AOPs) (Rueda-Márquez et al., 2015; Poyatos et al., 2010). An alternative to traditional treatment methods, advanced oxidation processes (AOPs) have been studied for the treatment of the wastewater that has been contaminated with oil. AOPs are distinguished by the employment of highly reactive intermediates called hydroxyl radicals ( $\bullet\text{OH}$ ), which attack and mineralize the organic contaminants in the wastewater. The two types of AOPs, homogeneous and heterogeneous, can be directed with or without light illumination. When iron atoms and hydrogen peroxide ( $\text{H}_2\text{O}_2$ ) interact with light, a standard photochemical process known as a homogeneous procedure takes place (Photo-Fenton) (Alkhazraji and Alatabe, 2021).

Heterogeneous photo-catalysis, which uses semiconductor catalysts ( $\text{ZnO}$ ,  $\text{TiO}_2$ ,  $\text{CdS}$ , and  $\text{Fe}_2\text{O}_3$ ), has demonstrated the ability to transform various potent and enigmatic organic materials into quickly biodegradable formulations as well as permanently mineralize them into inert elements like carbon dioxide and water (Malato et al., 2009). The Photo-Fenton, Fenton, UV, and  $\text{TiO}_2$  photo-catalytic processes were applied in the current study to treat an oily effluent at an oilfield (Alslaibi et al., 2014). The exact surface area of nano-dimensional  $\text{TiO}_2$  supports well-organized charge separation and charge trickery of ions on the  $\text{TiO}_2$  surfaces. The nano-sized  $\text{TiO}_2$  nanoparticles increased oxidative power with the associated aqueous phase opacity (Benhebal et al., 2013; Lee and Park, 2013). The employment of AOPs to remove organic pollutants is being debated by some researchers, including  $\text{ZnO}$  and  $\text{TiO}_2$  as solar photocatalysts (Maklavany et al., 2021) and oxidation of photo Fenton. Other researchers have used AOPs to remove phenol, mineralize (Khataee et al., 2019), and remove dyes from an aqueous medium. It was also employed to remove olive press residue (Campos et al., 2002; Chatzisyneon et al., 2013).

The main goal of this work was to separate the oil from generated water of Al-Khabaz Oilfield, North of Iraq, using (Homogeneous process) Fenton, photo Fenton, and photolysis (UV only). first, to find the efficient process that investigated high removal efficiency and second,

to study the impact of reagent dosage, the impact of light intensity, pH value, and irradiation period on the process. It is important to note that the removal of oil entails the degradation of all organic pollutants.

## EXPERIMENT

AOPs were used for the experimental work batch system process. The effects of pH, reaction time, UV lamp influence,  $\text{H}_2\text{O}_2$ ,  $\text{Fe}^{+2}$  concentrations, and  $\text{TiO}_2$  concentration were investigated.

### Materials

The chemicals utilized in this study are hydrogen peroxide (30% W/V, India),  $\text{Fe}^{+2}$  (India, 99 % purity),  $\text{NaCl}$  (India, 99.5 % purity),  $\text{NaOH}$  (98% purity, India),  $\text{H}_2\text{SO}_4$  (96% purity, Belgium) to modify the pH, and titanium dioxide (rutile) nanoparticle powder with a particle size of 20 to 30 nm (99% purity, Qingdao Hesiway).

The oil component of the generated water was extracted using (95% purity, India) an organic solvent n-Hexane ( $\text{CH}_3(\text{CH}_2)_4\text{CH}_3$ ), (95% purity, India). The Al-Khabaz oilfield in northern Iraq provided samples of the generated effluent. the water samples collected from the oil mentioned above were used in experiments and stored under conditions comparable to those in their natural environment that contained oxygen and other values to acquire a valuable treatment. The classification of produced water is shown in Table 1.

### Methods

#### *UV/H<sub>2</sub>O<sub>2</sub>/Fe<sup>+2</sup> batch reactor*

In this study, a batch reactor with a magnetic stirrer was used. It is a glass batch reactor in a UV chamber with (2–10) UV lamps, each with an output of eight watts and a wavelength of 365 nanometers (TL 8W BLB, Philips, Chine), which were used to conduct photo-Fenton experiments in a 250 ml glass beaker under ideal conditions.  $\text{Fe}^{+2}$  (2–20 mg) and  $\text{H}_2\text{O}_2$  (20–100 ml) were used at room temperature.

A pH range of 2.5–9.5 and an irradiation time of 30 to 120 minutes were used. Before adding the chemicals, 100 mL of the produced water was first poured into a 250 mL beaker, and the pH of the solution was adjusted using a pH meter (Model:

**Table 1.** Characteristics of the produced water

| Parameter           | Value                         |
|---------------------|-------------------------------|
| API at 60 °F        | 26.8                          |
| Calcium             | 0                             |
| Conductivity        | 84500 $\mu\text{s}/\text{cm}$ |
| Iron                | 0                             |
| Oil concentration   | 15.02 mg/l                    |
| Density at 60.08 °F | 1.12245 g/cm <sup>3</sup>     |
| Magnesium           | 1%                            |
| Sulphate            | 8945 mg/l                     |
| Sp.gr               | 1.1233                        |
| pH                  | 5.8                           |
| Phosphate           | 0.1031 mg/l                   |
| TDS                 | 54220 ppm                     |
| TSS                 | 31 mg/l                       |
| Turbidity           | 25.9                          |

pHep4 pH/temperature Tester-H1-98127). The experiment was started by turning on the UV lamps and the magnetic stirrer at 200 revolutions per minute to achieve a uniform blending of the solution in a glass beaker.

Following the experiment, a fine sample was obtained and examined with a UV spectrophotometer at 236 nm.

#### *Fe<sup>2+</sup>/H<sub>2</sub>O<sub>2</sub> batch reactor*

The same things of photo-Fenton were used in this process but without using UV lamps at room temperature and under optimal conditions. The magnetic stirrer was turned on at a speed of

200 rpm to begin the experiment. Following the investigation, a fine sample was obtained and examined with a UV spectrophotometer at 236 nm.

#### *Direct UV photolysis process (only UV) batch reactor*

Only UV (2–10) lamps were used in this step without adding any reagents, at room temperature and under optimal conditions. The UV lamps and magnetic stirrer were turned on and set to 200 revolutions per minute to begin the experiment. Following the investigation, the material was examined with a UV spectrophotometer at a wavelength of 236 nm.

#### *Photocatalytic heterogeneous method TiO<sub>2</sub>/UV*

FT-IR, XRD, and SEM experiments were used to study the characteristics of the catalyst titanium dioxide nanoparticles.

#### *Fourier transforms infrared spectroscopy*

The chemical composition and structural stability of the catalyst TiO<sub>2</sub> nanoparticles were investigated using Fourier transmission infrared spectroscopy (FT-IR). Figure 1 depicts the absorption values of the titanium dioxide sample, which range from (424.77 to 3403.71 cm<sup>-1</sup>)

#### *X-Ray diffraction analysis*

The pattern of XRD analysis is used to determine the crystalline phases of the titanium dioxide nanoparticle, revealing the information about

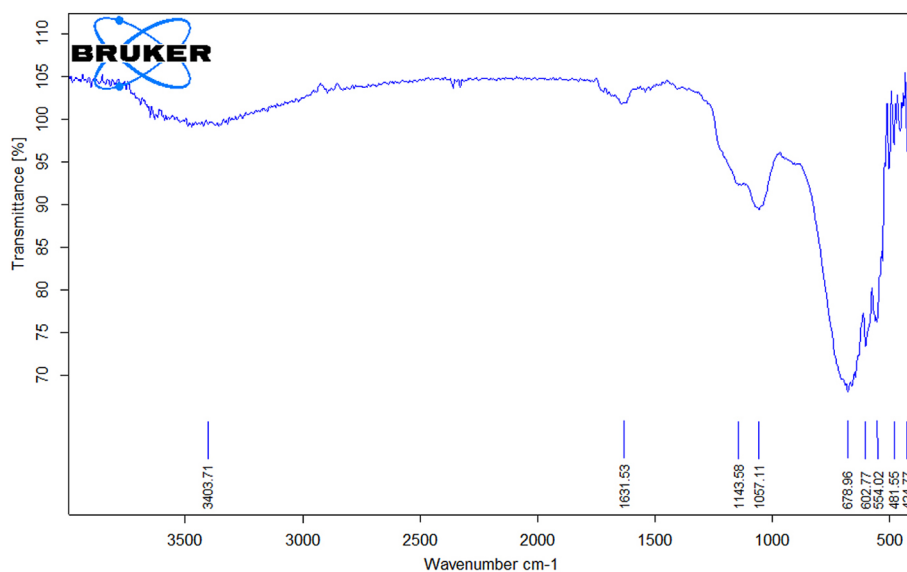


**Figure 1.** Fourier transforms infrared spectroscopy of TiO<sub>2</sub> NPs

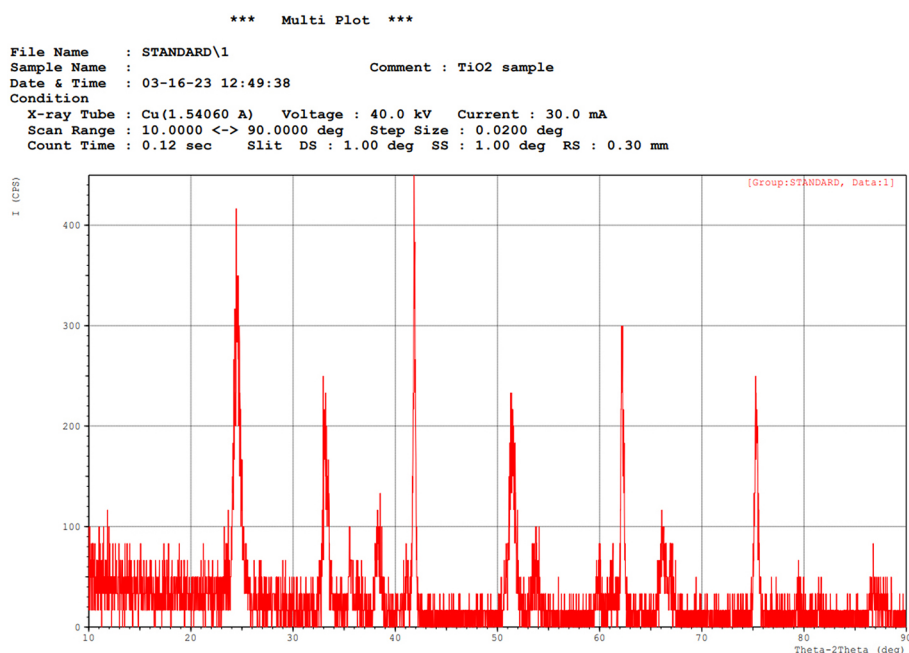


**Figure 2.** TiO<sub>2</sub> Nanoparticle x-ray diffraction pattern

its chemical structure, by studying the crystalline structure of the substance (Dubey et al., 2021; Dubey and Singh, 2017). Figure 2 depicts all of the obtained peaks.

#### Scan electron microscopy (SEM) analysis

The surface shape of the catalyst was determined by SEM examination of TiO<sub>2</sub> nanoparticles, which is one of the most important factors influencing photocatalysis performance. The SEM images reveal that the TiO<sub>2</sub> nanoparticles were equally produced and spherical, as shown in Figures 1, 2 and 3.

#### UV/TiO<sub>2</sub> nanoparticles batch reactor

In this technique, a batch reactor with a magnetic stirrer was used. Photocatalytic tests were carried out in a 250 ml glass beaker with a batch reactor in a UV chamber using UV lamps with an output of 8 watts and a wavelength of 365 nm (TL 8W BLB, Philips, China). Then, 25–75 mg of (TiO<sub>2</sub>) nanoparticles was used at ambient temperature. A pH range of 2.5–9.5 and an irradiation time of between 30 and 120 minutes were used. Before adding the TiO<sub>2</sub> nanoparticles catalyst, 100 mL of the generated water was placed into a 250 mL beaker, and the pH was adjusted. The UV lamps and magnetic stirrer were turned on and set to 200 revolutions per minute to begin the experiment. Following the experiment, a fine sample was obtained and examined with a UV

spectrophotometer at 236 nm. The experiments were carried out at room temperature. The effectiveness of removing oil from generated water was calculated using an efficiency equation.

$$\eta = \frac{C_{\text{initial}} - C_{\text{treated}}}{C_{\text{initial}}} \times 100 \% \quad (1)$$

where:  $\eta$  – oil removal efficiency,  $C_{\text{initial}}$  – the concentration of untreated oil (in ppm),  $C_{\text{treated}}$  – the concentration of treated oil (ppm).

The effluents were tested for oil concentration using the following process, which involved

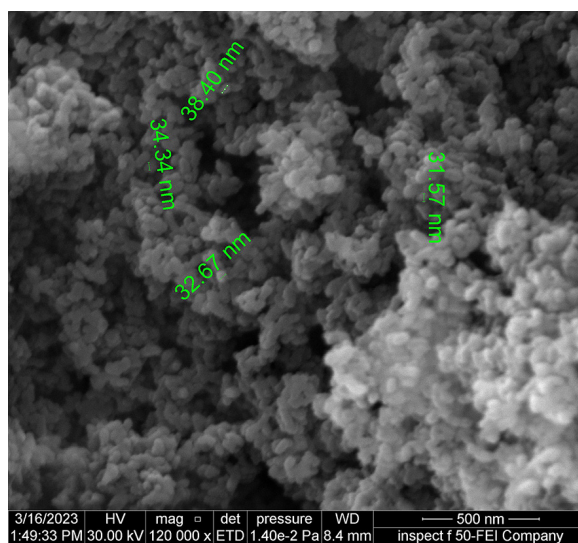


**Figure 3.** Scanning electron microscopic of TiO<sub>2</sub> nanoparticles

utilizing a spectrophotometer (GENESYS 10uv, USA) set to its maximum absorption wavelength of 236 nm. To dissolve the oil emulsion, 50 ml of generated water was mixed with 0.25 grams of NaCl salt in the separating funnel. After adding 5 ml of (n-Hexane), the mixture was shaken for 2 minutes. The solution was split into two layers after 20 minutes, the organic layer (upper layer) was utilized to determine the absorbance value, and then a standard curve was used to compute the oil content concentrations.

## RESULTS AND DISCUSSION

### Effect of UV irradiation time

The range of 30–120 minutes was tested for the influence of ultraviolet radiation on the amount of time needed to eliminate the organic contaminants found in generated water. Batch experiments investigated the link between irradiation time and oil removal effectiveness by photo-Fenton, direct

UV photolysis procedures, and photocatalytic process ( $\text{TiO}_2/\text{UV}$ ). Figure 4 shows the oil removal efficiency increased by increasing irradiation time and shows the highest removal rate was obtained at 120 min, which is the maximum irradiation time. This observation agreed with (Horng et al., 2009).

### Effect of pH value

In batch systems, the impact of pH at different values (ranging from 2.5 to 9.5) on the effectiveness of oil removal was investigated. Figure 5 illustrates the efficacy of oil removal at pH=2.5 and the efficiency decreasing at high pH values (the oxidation potential of free radicals ( $\bullet\text{OH}$ ) decreases with an increase in pH value) to achieve the highest efficiency possible. This is compatible with (Mota et al., 2008).

### Effect of hydrogen peroxide ( $\text{H}_2\text{O}_2$ ) doses

To find the optimal dose required for oil degradation in the produced water. Several experiments

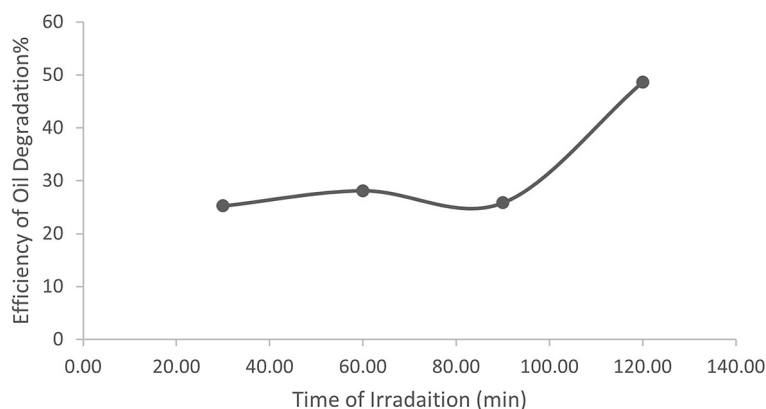


Figure 4. Effect of UV irradiation time

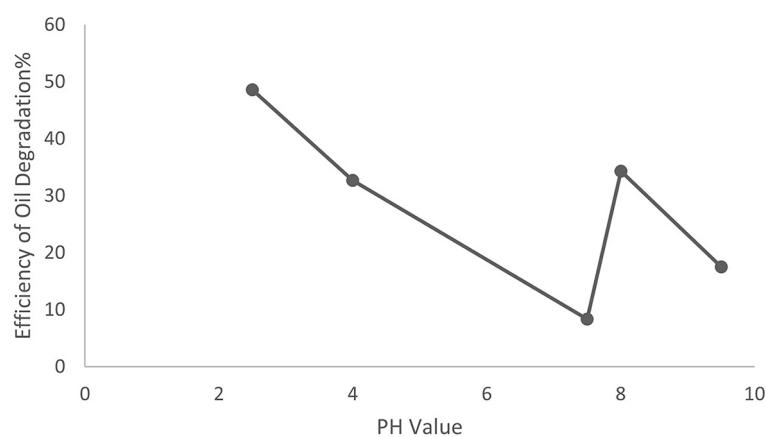


Figure 5. Effect of pH value

were conducted on the homogeneous Photo-Fenton and Fenton processes within doses (20–100) ml. The results presented in Figure 6 and Figure 7 show that the optimal amount is 20 ml (the highest removal efficiency achieved in this dose). An increase in  $H_2O_2$  does reduce the efficiency of oil removal in the Photo Fenton process as a result of the reactivity of free radicals ( $\bullet OH$ ) with excess hydrogen peroxide doses ( $H_2O_2$ ), this reaction will produce( $\bullet OH$ ). These radicals are inadequate compared to the ( $\bullet OH$ ) radicals (Al-atabe, 2018) the Fenton process observed, the oil degradation increases by 20 to 80 ml dose of  $H_2O_2$ . The optimal removal is achieved in a dose of 80 ml when the concentration of  $H_2O_2$  increases to 80 ml, and the degradation rate decreases. This is in accordance with (Tony et al., 2012).

### Effect of $Fe^{+2}$

Several tests were performed to investigate the impact of the ferrous sulfate ( $Fe^{+2}$ ) doses on the Photo-Fenton process and Fenton at the concentrations 2–18 mg. From Figure 8 and Figure 9,

it was concluded that when ferrous sulfate ( $Fe^{+2}$ ) doses increase, the oil removal efficiency gradually increases (the optimal amount was 18mg) for each process Fenton and photo-Fenton. This is following (Coha et al., 2021).

### Effect of UV intensity

In this study, the impact of the number of UV lamps on Photo-Fenton, direct UV photolysis, and photocatalytic ( $TiO_2/UV$ ) processes at (2–10) lamps (16–80 watt) was shown. Figure 10 demonstrates that the efficiency of oil removal decreases as the UV intensity increases in the photo-Fenton process (the best intensity is 16 watts (2 lamps)). Because the produced water was not exposed to any true primary treatment process, it may contain a variety of chemicals and ions that interact with reagents and oppose ultraviolet radiation, but in direct UV photolysis, and photocatalytic ( $TiO_2/UV$ ) processes the removal of oil increase with increasing in UV'S intensity as shown in Figure 11 and Figure 12. (Mitrović et al., 2012).

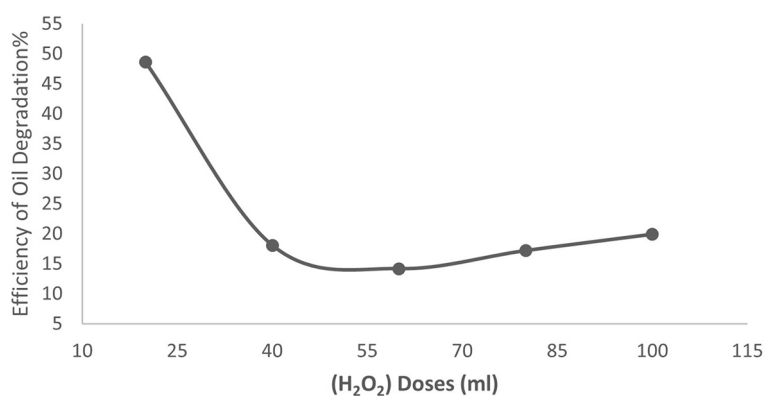


**Figure 6.** Photo-Fenton process – effect of hydrogen peroxide doses

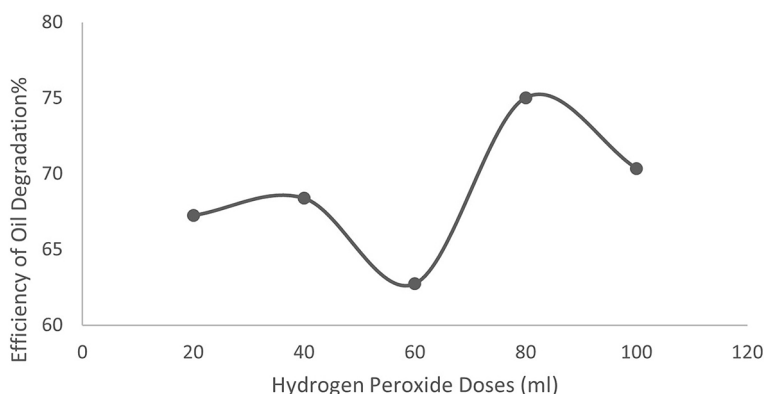


**Figure 7.** Fenton process – effect of hydrogen peroxide doses

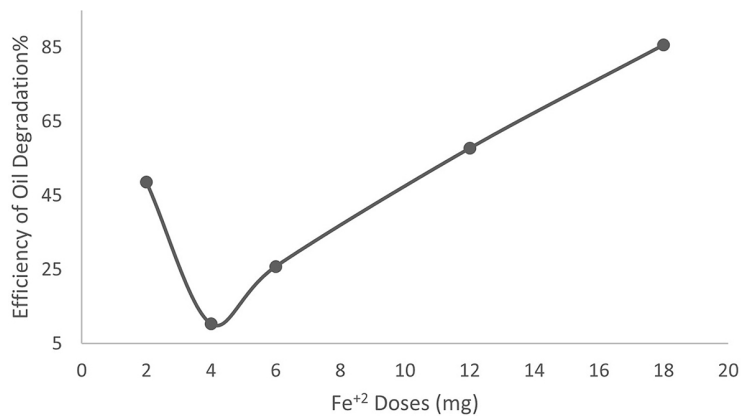


**Figure 8.** Impacts of Fe<sup>+2</sup> in Photo-Fenton process

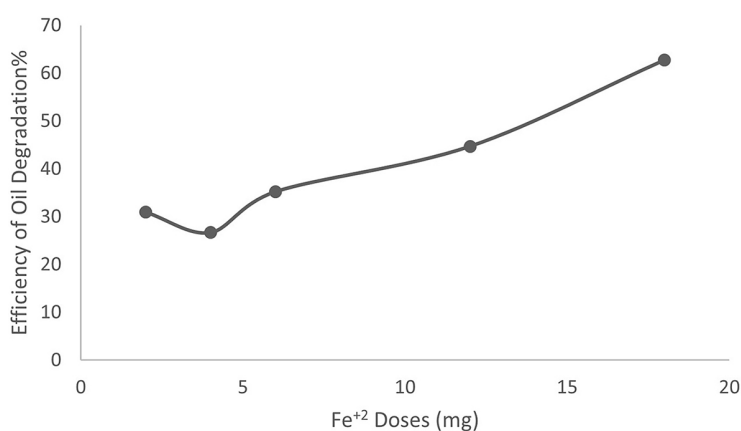


**Figure 9.** Impacts of Fe<sup>+2</sup> in Fenton process

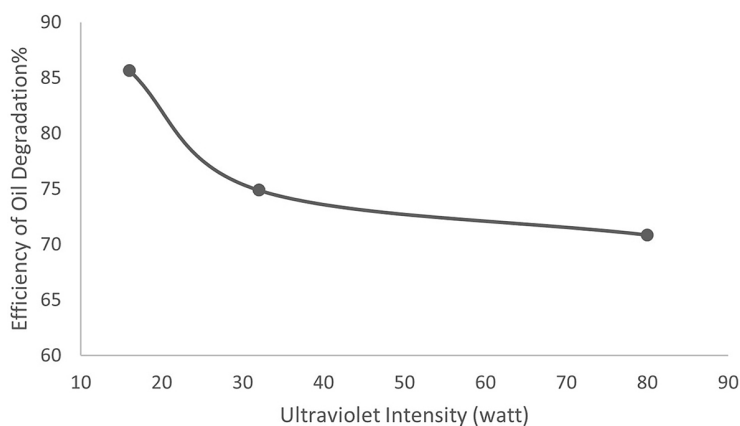


**Figure 10.** Photo-Fenton process – impacts of UV intensity

### Effect of TiO<sub>2</sub> nanoparticles doses

Several studies were performed to assess the effect of TiO<sub>2</sub> dosages ranging from 25 to 75 mg. Figure 13 shows that oil removal efficacy improved from 25 mg to to 55 mg to attain optimum elimination effectiveness; oil removal efficiency declined

above this value dose of TiO<sub>2</sub> nanoparticles. Excessive catalyst dosage will have a negative effect due to higher suspension, which prevents photon flux penetration and affinity for agglomeration, resulting in less surface area of catalyst available for light absorption and, as a result, a decrease in photocatalysis destruction rate. (Hassan and Al-Zobai, 2019).

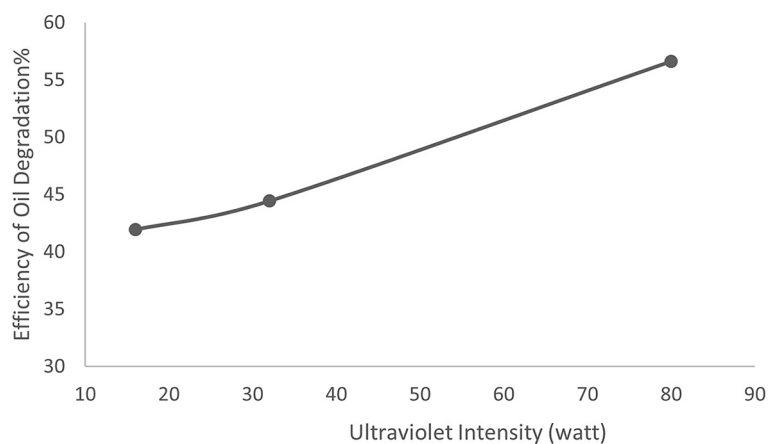


**Figure 11.** Direct UV process – impacts of UV intensity

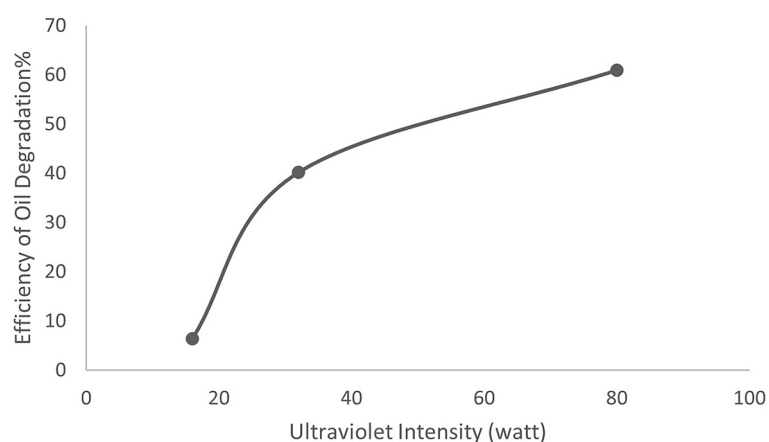


**Figure 12.** Photocatalytic process – impacts of UV intensity

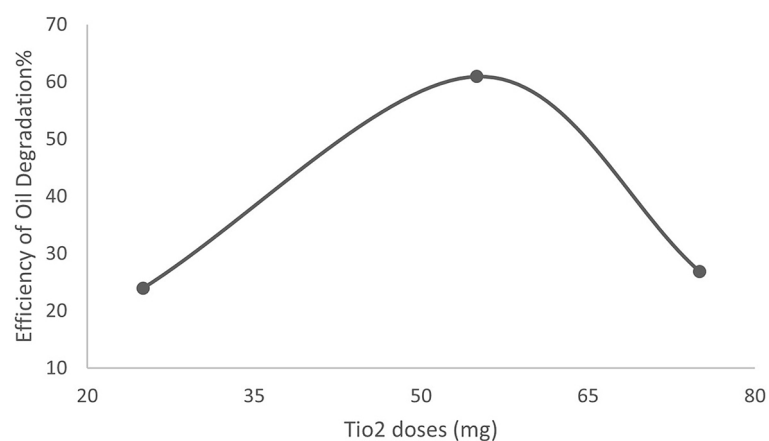


**Figure 13.** Photocatalytic process – impacts of (TiO<sub>2</sub>) nanoparticles doses

## CONCLUSIONS

This work used sophisticated oxidation techniques, including homogeneous (Fenton, photo-Fenton, and UV photolysis processes) and heterogeneous catalytic TiO<sub>2</sub> nanoparticles for batch

processing, to explore the separation of oil from the oilfield wastewater in the Al Khabaz oilfield in northern Iraq. The glass reactor was used for this operation, and the best conditions were used for the most effective oil removal. The outcomes of the experimental work demonstrate that



photo-Fenton oxidation is a successful treatment method. The effects of irradiation time, pH, H<sub>2</sub>O<sub>2</sub> & Fe<sup>+2</sup> dosages, the intensity of UV, and TiO<sub>2</sub> concentrations were studied; the results show that the effective way to remove oil was achieved in the Photo-Fenton process, approximately = 85.68% of oil content was degraded in a reaction time of 2 hours. FT-IR, SEM and XRD tests were studied to investigate the properties of the catalyst titanium dioxide nanoparticles. The results showed absorption values of the TiO<sub>2</sub> sample in FT-IR analysis varied from 424.77 to 3403.71 cm<sup>-1</sup>, TiO<sub>2</sub> NPs had a spherical appearance with sizes ranging from 31.57 to 38.40 nm, and XRD got details about the structure of the titanium dioxide.

### Acknowledgements

The authors express thanks to the Department of Environmental Engineering at Mustansiriyah University for their investigative services.

### REFERENCES

1. Al-atabe M.J.A. 2018. A Novel Approach for Adsorption of Copper(II) Ions from Wastewater Using Cane Papyrus. *International Journal of Integrated Engineering*, 10(1), 96–102. <https://doi.org/10.30880/IJIE.2018.10.01.015>
2. Alatabe M.J.A., Hameed M.A.R., Al-zobai K.M.M. 2021. Exfoliate apricot kernels, natural low-cost bio-sorbent for rapid and efficient adsorption of CN<sup>-</sup> ions from aqueous solutions. Isotherm, kinetic and thermodynamic models. *International Journal of Applied Science and Engineering*, 18(5), 1–11. [https://doi.org/10.6703/ijase.202109\\_18\(5\).003](https://doi.org/10.6703/ijase.202109_18(5).003)
3. Alkhazraji H.A., Alatabe M.J. 2021. Oil Recovery from Oilfield Produced Water Using Zink Oxide Nano Particle as Catalyst in Batch and Continuous System. *Journal of Ecological Engineering*, 22(8), 278–286. <https://doi.org/10.12911/22998993/140281>
4. Alslaibi T.M., Ismail A., Mohd A.A., Ahmed A.F. 2014. Heavy metals removal from wastewater using agricultural wastes as adsorbents: a review. *International Journal of Chemical and Environmental Engineering*, 5(1), 7–10.
5. Benhebal H., Chaib M., Salmon T., Geens J., Leonard A., Lambert S.D., Crine M., Heinrichs B. 2013. Photocatalytic degradation of phenol and benzoic acid using zinc oxide powders prepared by the sol-gel process. *Alexandria Engineering Journal*, 52(3), 517–523. <https://doi.org/10.1016/j.aej.2013.04.005>
6. Campos J.C., Borges R.M.H., Oliveira Filho A.M. de, Nobrega R., Sant'Anna Jr G.L. 2002. Oilfield wastewater treatment by combined microfiltration and biological processes. *Water Research*, 36(1), 95–104.
7. Chatzisyneon E., Foteinis S., Mantzavinos D., Tsoutsos T. 2013. Life cycle assessment of advanced oxidation processes for olive mill wastewater treatment. *Journal of Cleaner Production*, 54, 229–234. <https://doi.org/10.1016/j.jclepro.2013.05.013>
8. Coxa M., Farinelli G., Tiraferri A., Minella M., Vione D. 2021. Advanced oxidation processes in the removal of organic substances from produced water: Potential, configurations, and research needs. *Chemical Engineering Journal*. Elsevier B.V., 414. <https://doi.org/10.1016/j.cej.2021.128668>
9. Dubey R.S., Jadkar S.R., Bhorde A.B. 2021. Synthesis and Characterization of Various Doped TiO<sub>2</sub> Nanocrystals for Dye-Sensitized Solar Cells. *ACS Omega*, 6(5), 3470–3482. <https://doi.org/10.1021/acsomega.0c01614>
10. Dubey R.S., Singh S. 2017. Investigation of structural and optical properties of pure and chromium doped TiO<sub>2</sub> nanoparticles prepared by solvothermal method. *Results in Physics*, 7, 1283–1288. <https://doi.org/10.1016/j.rinp.2017.03.014>
11. Hadi H.J., Al-zobai K.M.M., Alatabe M.J.A. 2020. Oil Removal from Produced Water using Imperata cylindrica as Low-Cost Adsorbent. *Current applied science and technology*, 494–511.
12. Hassan A.A., Al-Zobai K.M.M. 2019. Chemical oxidation for oil separation from oilfield produced water under uv irradiation using titanium dioxide as a nano-photocatalyst by batch and continuous techniques. *International Journal of Chemical Engineering*, 2019. <https://doi.org/10.1155/2019/9810728>
13. Horng R.Y., Huang C., Chang M.C., Shao H., Shiau B.L., Hu Y.J. 2009. Application of TiO<sub>2</sub> photocatalytic oxidation and non-woven membrane filtration hybrid system for degradation of 4-chlorophenol. *DES*, 245, 169–182. <https://doi.org/10.1016/j.desal.2009.04.003>
14. Jabbar H.A., and Alatabe M.J.A. 2021. Treatment Oilfield Produced Water using Coagulation/Flocculation Process (case study: Alahdab Oilfield). *Pollution*, 7(4), 787–797.
15. Khataee A., Kalderis D., Gholami P., Fazli A., Moschogiannaki M., Binas V., Lykaki M., and Konsolakis M. 2019. Cu<sub>2</sub>O-CuO@ biochar composite: synthesis, characterization and its efficient photocatalytic performance. *Applied Surface Science*, 498, 143846.
16. Lee S.Y., Park S.J. 2013. TiO<sub>2</sub> photocatalyst for water treatment applications. In *Journal of Industrial and Engineering Chemistry*, 19(6), 1761–1769. <https://doi.org/10.1016/j.jiec.2013.07.012>
17. Lekomtsev A.V., Mordvinov V.A., Ilyushin P.Y., Bakaneev V.S., Kornilov K.V. 2021. Centrifugal Separation in the Treatment of Produced Water for

- its Subsequent Injection into a Reservoir. *Chemical and Petroleum Engineering*, 56(11–12), 979–987. <https://doi.org/10.1007/s10556-021-00872-6>
18. Maklavany D.M., Rouzitalab Z., Jafarnejad S., Mohammadpourderakhshi Y., Rashidi A. 2021. Application of Copper Oxide-Based Catalysts in Advanced Oxidation Processes. *Applied Water Science: Remediation Technologies*, 2, 485–525.
  19. Malato S., Fernández-Ibáñez P., Maldonado M.I., Blanco J., Gernjak W. 2009. Decontamination and disinfection of water by solar photocatalysis: Recent overview and trends. In *Catalysis Today*, 147(1), 1–59. <https://doi.org/10.1016/j.cattod.2009.06.018>
  20. Mitrović J., Radović M., Bojić D., Anbelković T., Purenović M., Bojić A. 2012. Decolorization of the textile azo dye Reactive Orange 16 by the UV/H<sub>2</sub>O<sub>2</sub> process. *Journal of the Serbian Chemical Society*, 77(4), 465–481. <https://doi.org/10.2298/JSC110216187M>
  21. Mohanakrishna G., Al-Raoush R.I., Abu-Reesh I.M. 2021. Integrating electrochemical and bioelectrochemical systems for energetically sustainable treatment of produced water. *Fuel*, 285, 119104.
  22. Mota A.L.N., Albuquerque L.F., Beltrame L.T.C., Chiavone-Filho O., Machulek A., and Nascimento C.A.O. 2008. Brazilian journal of petroleum and gas advanced oxidation processes and their application in the petroleum industry: a review. *Brazilian Journal of Petroleum and Gas*, 3, 122–142.
  23. Mustafa Y., Alwarded A.I., Abdulaziz M., Mothana E.Y. 2013. Removal of oil from wastewater by advanced oxidation process/homogeneous process. The kinetics and modeling of advanced oxidation processes View project I am working on CO<sub>2</sub> emission and its effects in climate change in Iraq View project Removal of oil from wastewater by advanced oxidation process / homogeneous process. *Journal of Engineering*, 19(6). <https://www.researchgate.net/publication/331473196>
  24. Poyatos J.M., Muñio M.M., Almecija M.C., Torres J.C., Hontoria E., Osorio F. 2010. Advanced oxidation processes for wastewater treatment: State of the art. *Water, Air, and Soil Pollution*, 205(1–4), 187–204. <https://doi.org/10.1007/s11270-009-0065-1>
  25. Rana A.G., Tasbihi M., Schwarze M., Minceva M. 2021. Efficient Advanced Oxidation Process (AOP) for Photocatalytic Contaminant Degradation Using Exfoliated Metal-Free Graphitic Carbon Nitride and Visible Light-Emitting Diodes. *Catalysts*, 11(6), 662.
  26. Rueda-Márquez J.J., Sillanpää M., Pocostales P., Acevedo A., Manzano M.A. 2015. Post-treatment of biologically treated wastewater containing organic contaminants using a sequence of H<sub>2</sub>O<sub>2</sub> based advanced oxidation processes: Photolysis and catalytic wet oxidation. *Water Research*, 71, 85–96. <https://doi.org/10.1016/j.watres.2014.12.054>
  27. Shawkat A.A., Rashad Z.W., Rashad A.A., Kareem N.A.A., Abbas T.K., Alsahy Q.F., Abbas A.D., Sherhan B.Y. 2016. Produced Water Treatment Using Ultrafiltration and Nanofiltration Membranes. *Al-Khwarizmi Engineering Journal*, 12(3), 10–18.
  28. Tetteh E.K., Rathilal S., Naidoo D.B. 2020. Photocatalytic degradation of oily waste and phenol from a local South Africa oil refinery wastewater using response methodology. *Scientific Reports*, 10(1). <https://doi.org/10.1038/s41598-020-65480-5>
  29. Tony M.A., Purcell P.J., Zhao Y. 2012. Oil refinery wastewater treatment using physicochemical, Fenton and Photo-Fenton oxidation processes. *Journal of Environmental Science and Health - Part A Toxic/Hazardous Substances and Environmental Engineering*, 47(3), 435–440. <https://doi.org/10.1080/10934529.2012.646136>
  30. Villegas L.G.C., Mashhadi N., Chen M., Mukherjee D., Taylor K.E., Biswas N. 2016. A short review of techniques for phenol removal from wastewater. *Current Pollution Reports*, 2(3), 157–167.